Physicochemical characterization and adsorption behavior of Ca/Al chloride hydrotalcite-like compound towards removal of nitrate

Mahamudur Islam [a,*], Rajkishore Patel [b]

[a] Department of Chemistry, Purushottam Institute of Engineering & Technology, Purushottam Vihar, 10th km, Highway – 10, Mandiakudar, Kansbahal, Rourkela 770034, Orissa, India
[b] Department of Chemistry, National Institute of Technology, Rourkela 769008, Orissa, India

ARTICLE INFO

ABSTRACT

The objective of the present research was to synthesize, characterize and to investigate adsorption of nitrate from synthetic nitrate solution by Ca–Al–Cl HTlc. In the present study Ca–Al–Cl HTlc was synthesized by co-precipitation method and was characterized using SEM, XRD, FTIR and TGA–DSC. To assess the practical usefulness, a detailed removal study of nitrate was carried out. The removal of nitrate was 84.6% under neutral condition using 0.35 g of adsorbent in 100 mL of nitrate solution having initial concentration of 10 mg/L. Adsorption kinetic study revealed that the adsorption process followed first order kinetics. Adsorption data were fitted to linearly transformed Langmuir adsorption isotherm with R^2 (correlation coefficient) > 0.99. Thermodynamic parameters were also calculated to study the effect of temperature on the removal process. In order to understand the adsorption type, equilibrium data were tested with Dubinin–Radushkevich isotherm.

© 2011 Elsevier B.V. All rights reserved.

1. Introduction

Hydrotalcites, also known as layered double hydroxides or ionic clays are based upon the brucite [Mg(OH)2] structure in which some of the divalent cations are replaced by trivalent cations (e.g. Al^{3+}, Fe^{3+}, Cr^{3+}, etc.) resulting in a layer charge. This layer charge is counter balanced by anions such as carbonate, nitrate, sulphate or chloride in the interlayer spaces. In hydrotalcites a broad range of compositions of the type $[M_{1-x}^{2+}M_x^{3+} (OH)_2][A^{n-}]_{x/n} \cdot yH_2O$ are possible, where M^{2+} and M^{3+} are the di and trivalent cations in the octahedral positions within the hydroxide layers with x normally between 0.17 and 0.33. A^{n-} is an exchangeable interlayer anion [1]. The degree of anionic replacement in the hydrotalcites depends on the structural characteristics, e.g. the nature of the interlayer anion and crystallinity. Exchange conditions like pH and carbonate contamination from environment are also important limitations. Due to the high affinity of hydrotalcites towards carbonate ion, materials with intercalated carbonate ions have relatively smaller exchange capacities unless being calcined. High pH conditions must be applied to maintain the stability of hydrotalcites, however, OH^- intercalation is competitive in this case. The technological applications of hydrotalcite and calcined hydrotalcite have attracted much attention in recent years [2–5].

Hydrotalcite-derived mixed oxides are used as antacids, catalysts and catalyst supports, because of their high surface area, phase purity, basic surface properties, and structural stability [5]. Hydrotalcite-derived oxides catalyze higher alcohol synthesis from CO/H_2 [6], oxidation of mercaptans [7] and water gas shift reactions [8]. Also, Mg–Al mixed oxides prepared by oxidative decomposition of hydrotalcite precursors have been used in base-catalyzed aldol condensations [9,10], alkylations [11], Knoevenagel condensations [12], double-bond isomerization, and alcohol dehydrogenation and coupling. There are many other important uses of hydrotalcites such as in the removal of environmental hazards in acid mine drainage [13,14] and a mechanism for the disposal of radioactive wastes [15]. The use of hydrotalcites as ion exchangers and adsorbents has drawn the attention of researchers.

Among the many uses is the removal of toxic anions from aqueous systems. Nitrate in water is quite harmful in food and drinks of young children and can be quite toxic. Nitrate is a wide spread contaminant of ground and surface water due to excessive use of nitrogenous fertilizer in agricultural activities and disposal of untreated sanitary and industrial wastes [16–18]. Elevated nitrate concentrations in drinking water are linked to health problems such as methemoglobinemia in infants and stomach cancer in adults. US Environmental Protection Agency (EPA) has set the maximum contamination level as 44 mg/L of NO_3^- [19,20]. Current technologies for removal of nitrate, like ion-exchange and reverse osmosis, are not selective to nitrate, generate secondary brine wastes and require frequent media regeneration. In recent years chemical methods of nitrate removal using zero-valent metals like iron (Fe^0),

magnesium (Mg^0) and aluminum (Al^0) has been studied intensively [21–27]. However, challenges like high dose requirement, long reaction time, presence of anaerobic condition and rapid deactivation of metal surface due to hydroxide precipitation. The use of biological reactor seems to be the most promising technique in the treatment of high nitrate concentration. However, maintaining biological processes at their optimum conditions is difficult, and the problems of contamination by bacteria [28] have to be solved to make such processes safe enough to utilize for drinking water treatment. On the other hand, adsorption is a very feasible process but there are not many adsorbent available for removal of nitrate since nitrate is very selective towards adsorption. Among a few adsorbents, hydrotalcite like compounds may prove beneficial for adsorption of nitrate.

Although few studies have examined the synthesis of various HTlcs and the way in which they interact with various anions, the synthesis of Ca/Al chloride hydrotalcite and its application for efficient removal of nitrate has not been examined previously. So, the present research was aimed to synthesize and characterize Ca/Al chloride hydrotalcite. The effect of various parameters on the effectiveness of treating nitrate contaminated water with Ca/Al chloride was unknown. Therefore, in this study, Ca/Al chloride was added to nitrate solutions and the effect of different variables (calcinations temperature, dose, time, pH, initial nitrate concentration, effect of other anions, etc.) on the removal of nitrate from solution by Ca/Al chloride was examined.

2. Experimental

2.1. Reagents and chemicals

Potassium nitrate used in the present study was of analytical grade and was obtained from Merck. 1000 mg/L stock solution of nitrate was prepared by dissolving 1.6305 g of KNO_3 in 1 L distilled water. The required concentration of nitrate solution was obtained by serial dilution of 1000 mg/L nitrate solution. The measuring cylinder, volumetric flask and conical flask used were of Borosil.

2.2. Synthesis of Ca/Al chloride hydrotalcite

Ca–Al–Cl hydrotalcite was prepared by co-precipitation method at pH 10 [29]. In this method two solutions, solution-I containing 0.75 M $CaCl_2$ and 0.25 M $AlCl_3$ and solution-II containing 1 M NaOH and 1 M NaCl, 200 ml each of these two solutions were added simultaneously to a 1 L beaker containing 100 mL of distilled water at a flow rate of 50 mL per hour at 80 °C under vigorous stirring. An inert atmosphere was maintained throughout the addition by bubbling nitrogen gas from a cylinder. The pH of the solution was maintained at 10 by the addition of 2 M NaOH. The slurry was then refluxed at 90 °C for 24 h. It was then filtered and washed thoroughly with distilled water till the washings were neutral. The precipitate was then dried in nitrogen atmosphere for 8 h. The HTlc obtained was calcined at different temperature (50–400 °C) in nitrogen atmosphere for 8 h.

2.3. Characterization of Ca/Al chloride hydrotalcite

BET surface area of the sample was measured using QUAN-TACHROME Autosorb I. The sample was degassed at 100 °C in vacuum. Helium was used as carrier gas and the surface area was measured by nitrogen adsorption–desorption method at liquid nitrogen temperature. Thermogravimetric analysis and differential scanning calorimetry (TGA/DSC) was carried out using NETZSCH STA 409C. 30 mg of the sample was used and alumina was used as reference. TGA and DSC curve was obtained from 25 °C to 800 °C at

Table 1
Synthesis of various samples of hydrotalcite like compounds (HTlcs).

Uncalcined layered double hydroxides (LDHs)	Percentage removal of nitrate from 100 mg/L solution
Ca–Al–Cl	65.2
Mg–Al–CO_3	3.6
Zn–Cr–Cl	11.2
Mg–Mn–CO_3	3.8
Mg–Cr–Cl	9.8
Ca–Cr–Cl	5.2

a rate of 10 °C/min. Scanning electron micrographs of the sample was obtained by JEOL JSM – 6480LV scanning electron microscope. The sample was coated with platinum for 30 s at a current of 50 mA before the SEM micrograph was obtained. Chemical analysis of HTlc was carried out by dissolving 0.5 g of material in 1:1 HCl, followed by the estimation of Al by precipitating it with NH_4Cl and NH_4OH. Then the residual solution contained Ca which was estimated by standard EDTA [29,30]. Powder XRD of the material was obtained by using PHILLIPS X'PERT X-Ray diffractometer with Cu Kα radiation (35 kV and 30 mA) at a scan rate of 1°/min and was analyzed using standard software provided with the instrument. FTIR of the sample was obtained using Perkin Elmer FTIR spectrophotometer (SPECTRUM RX – I).

2.4. Batch experiments

The nitrate removal experiments from its aqueous solution by HTlc were carried out using standard 10 mg/L, 50 mg/L and 100 mg/L NO_3^-. The adsorption experiments were carried out in 250 mL glass conical flask with stopper by adding 0.1–0.8 g of HTlc in 100 mL of synthetic nitrate solution. Stoppers were provided to avoid change in concentration due to evaporation. All the experiments were carried out at ambient temperature (25 ± 2 °C). After continuous stirring over a magnetic stirrer at about 400 rpm for a predetermined time interval, nitrate concentration was determined by Nitrate ion selective electrode (Orion Ionplus Sureflow Nitrate Electrode) and Orion 720 A+ ion analyzer. Two standards were prepared that bracket the expected sample range and which differ in concentration by a factor of ten. Measurements were done by taking 10 mL of each standard and sample into separate 50 mL beaker and 10 mL of nitrate interference suppressor (930710). All the sample and standards were maintained at same temperature to avoid interference due to difference in temperature. A number of parameters such as reaction time, adsorbent dose, concentration of nitrate, pH, affecting the removal of nitrate ion have been varied widely in order to optimize the removal process.

3. Results and discussion

3.1. Characterization

A number of HTlc samples were prepared and examined for the removal efficiency of nitrate. This was done by adding a 0.5 g sample of each HTlc to 100 mg/L nitrate solution, stirring for 8 h, filtering the solution and analyzing for residual nitrate. The result of the study is presented in Table 1. The percentage removal of nitrate was 65.2% for Ca–Al–Cl. It is evident from the table that Ca–Al–Cl exhibited maximum removal of nitrate from synthetic nitrate solution. All other HTlcs used, exhibited poor nitrate removal efficiency (less than 12%). So, Ca–Al–Cl was selected for further study.

To study the effect of calcination temperature on the removal of nitrate, sample of Ca–Al–Cl HTlc was calcined at different temperatures (50–400 °C in nitrogen atmosphere) for 8 h. 0.5 g of calcined samples were added to 100 mL of 100 mg/L nitrate solution and percentage removal of nitrate was studied. The result of the study

Table 2
Effect of calcinations temperature on the removal of nitrate by various samples of hydrotalcite like compounds (HTlcs).

Calcination temperature (in °C)	Percentage removal of nitrate from 100 mg/L synthetic nitrate solution by Ca–Al–Cl
50	65.2
100	68.3
150	70.8
200	74.7
250	73.2
300	60.2
350	52.2
400	40.7

is presented in Table 2. It is clear from the table that the percentage removal increased with increase in temperature up to 200 °C and then it started to decrease. Maximum removal of 74.7% was obtained with Ca–Al–Cl calcined at 200 °C. So, the above HTlc was calcined at 200 °C and were used for batch studies.

Specific surface area of HTlc calcined at different temperature was measured using QUANTACHROME Autosorb-I. Result of the study is presented in Fig. 1. It is evident from the figure that the specific surface area (BET) increased with increase in calcination temperature. It was observed that, there was rapid increase in BET surface area of HTlc with increase in calcination temperature from 100 °C to 200 °C and there was slight increase in BET surface area with increase in calcinations temperature beyond 200 °C. The BET surface area of HTlc calcined at 200 °C was 191.3 m²/g. Though there was further increase in specific surface area with increase in calcination temperature, the percentage removal of nitrate decreased after calcination at 200 °C (Fig. 1). This may be due to the structural deformation of HTlcs, which takes place when calcined at higher temperature [29]. So, material was calcined at 200 °C and batch studies were carried out.

The electrophoretic studies are important in view of determination of behavior of adsorbent materials in different electrolytic medium. The point of zero charge (pH_{pzc}) was determined using electrophoretic mobility in a solution of ionic strength 0.01 M NaCl and 0.001 M NaCl (Fig. 2). The point at which the zeta potential was found to be zero is termed as point of zero charge. From the electrophoretic studies shown graphically as a function of pH versus the zeta potential in mV (Fig. 2), the point of zero charge values of Ca–Al–Cl HTlc was found to be 7.5 at both 0.01 M and 0.001 M NaCl solution.

TGA and DSC analysis of HTlc were carried out and results are presented in Fig. 3. The DSC study of Ca–Al–Cl HTlc revealed
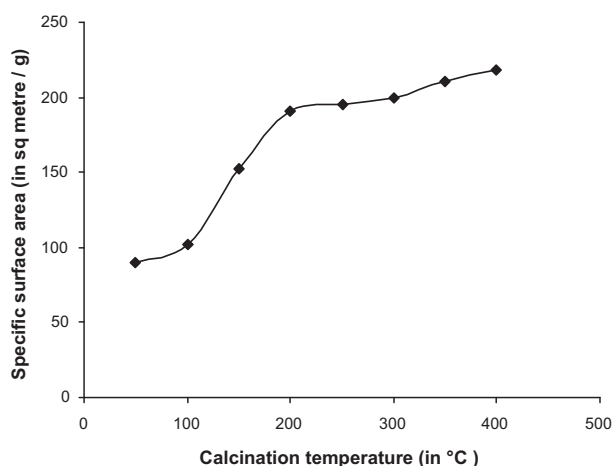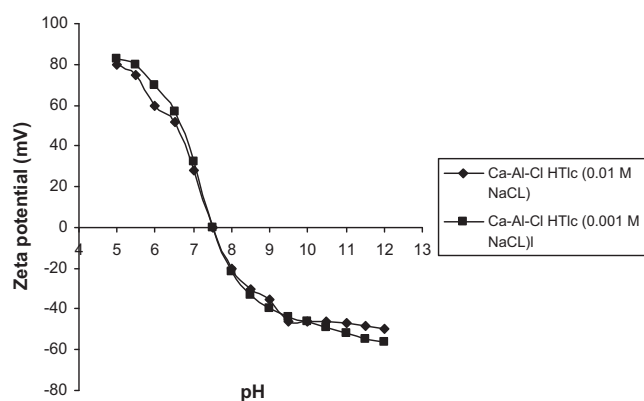
Fig. 2. Zeta potential of Ca–Al–Cl HTlc as a function of pH using 0.01 M NaCl and 0.001 M NaCl as supporting electrolyte.

that there were three endothermic peaks. First, second and third endothermic processes were up to the temperature of 159.35 °C, 291.35 °C and 799.35 °C, respectively. The endothermic process up to 159.35 °C may be due to the loss of physically adsorbed water molecules. Weight loss up to 159.35 °C was calculated from the TGA analysis and was found to be 6.562%, which corresponds to the percentage of physically adsorbed water present in the HTlc. The second endothermic process, which continued up to 291.35 °C, may be attributed to loosely bound water in the interlayer spaces of the HTlc. The corresponding weight loss from the TGA curve was found to be 12.942% and the weight loss by the end of third endothermic process (up to 799.35 °C) was found to be 21.006%. It is due to the simultaneous dehydroxylation of lattice OH⁻ and strongly bound water.

Scanning electron micrograph of Ca–Al–Cl HTlc sample was obtained and is presented in Fig. 4. The structural morphology of the HTlc can be clearly observed from the figure. Chemical analysis of HTlc were carried out in order to calculate the molar ratios of M^{II}:M^{III} present in the HTlc. During the synthesis, M^{II}:M^{III} ratio was taken as 3:1. The Ca:Al ratios was found to be 2.987:1. The M^{II}:M^{III} ratios obtained were very close to 3:1. So, chemical analysis of HTlc ascertains the synthesis with required M^{II}:M^{III} ratios. The chemical formula, on the basis of chemical analysis can be suggested as $[Ca_3Al(OH)_8]Cl \cdot xH_2O$.

Powder XRD of HTlc (before and after adsorption) was obtained and the graph is presented in Fig. 5. The diffractogram was analyzed with Philips X'Pert High Score software to search for the phases of
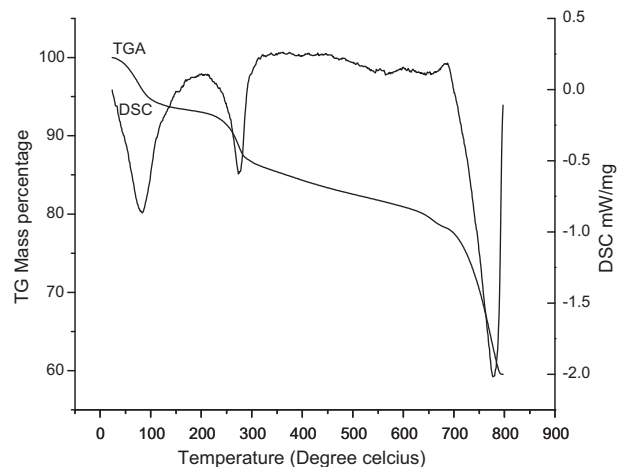
Fig. 1. Specific surface area of Ca–Al–Cl HTlc calcined at different temperatures.

Fig. 3. Thermogravimetric analysis and differential scanning calorimetry of Ca–Al–Cl layered double hydroxide.

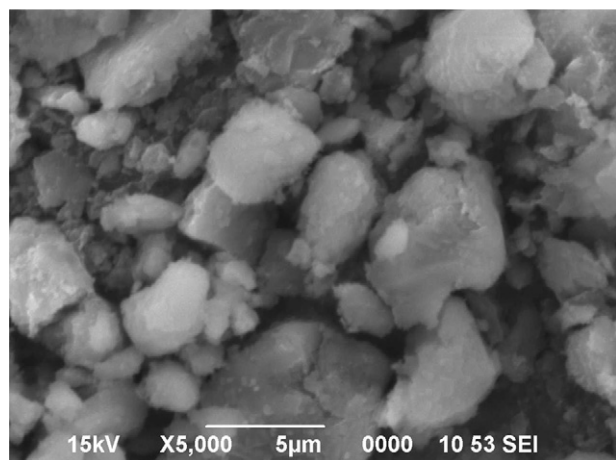**Fig. 4.** SEM micrograph of Ca–Al–Cl layered double hydroxide (magnification – 5000×, 15 kV).

Fig. 6. FTIR pattern of Ca–Al–Cl layered double hydroxide and Ca–Al–Cl LDH recovered after adsorption.

starting materials. The result obtained from the analysis indicated that there was not any starting materials present in the HTlc. Fig. 5 shows sharp and symmetric peaks which gives clear indication that the samples are well crystalline and peak corresponding to (0 0 3), (0 0 6), (1 1 0), and (1 1 3) planes are characteristic of clay minerals (HTlc) having layered structure. Diffraction peaks of nitrate containing material were found in the XRD analysis of HTlc obtained after nitrate adsorption. This may be due to the nitrate adsorption by the material.

FTIR study of Ca–Al–Cl HTlc and HTlc recovered after adsorption were carried out in order to know the presence of different groups, structures and adsorption of nitrate onto HTlc. FTIR spectrum of Ca–Al–Cl is presented in Fig. 6. An intense broad band at 3470 cm^{-1} may be due to superimposition of deformational vibrations of physically adsorbed water [31], vibrations of structural OH$^-$ groups [32] and characteristic valent vibration of HO···OH in hydrotalcite [33]. The band at 2361 cm^{-1} is apparently due to CO$_2$ background of the measurement system [34]. The band at 1636 cm^{-1} (bending vibration of δ HOH) may be assigned to the adsorbed interlayer water. The band at 1474 cm^{-1} is most probably due to carbonate anion, which might have formed due to absorption of atmospheric CO$_2$ gas. The bands at 712 cm^{-1} and 668 cm^{-1} coincide by position and intensity ratio with the characteristic vibrations of hydrotalcite [33]. FT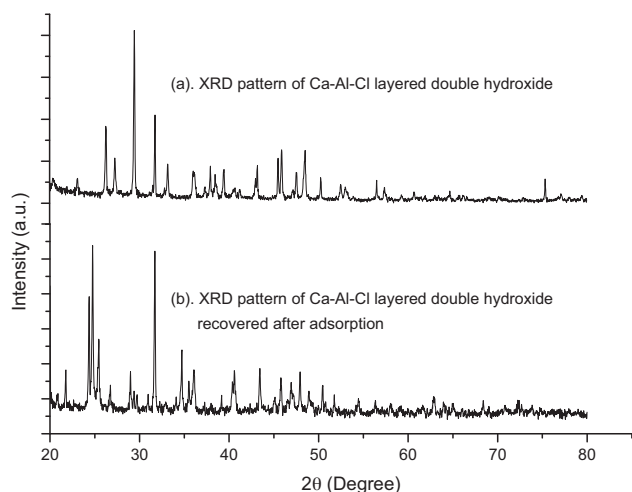IR spectrum of Ca–Al–Cl recovered after adsorption is presented in Fig. 6. A band at 3465 cm^{-1} was observed, which may be due to physically adsorbed water [31], vibrations of structural OH$^-$ groups [32]. A band at 2364 cm^{-1} is due to CO$_2$ background of the measurement system. Band at 1636 cm^{-1} (bending vibration of δ HOH) may be due to the adsorbed interlayer water. A band at 1384 is associated with the antisymmetric stretching mode of nitrate (v_3) [35,36] which ascertains the adsorption of nitrate onto Ca–Al–Cl HTLC. The bands at 712 and 671 cm^{-1} correspond to the characteristic vibrations of hydrotalcite.

The calcined material was used to remove nitrate from ground water samples collected from six different bore wells. The study was carried out at ambient temperature ($25 \pm 2\,^\circ$C) and for a contact time of 30 min, with 0.35 g of the material in 100 mL of sample water. The result of the study is presented in Table 3. It is evident from the table that the percentage removal was within the range of 69–81%. The final nitrate concentration of the treated sample water was within the permissible limit (44 mg/L). So, it is evident from the study that the material can be efficiently used to remove nitrate from real ground water.

3.2. Removal study of nitrate by batch mode experiments

3.2.1. Effect of adsorbent dose

The effect of variation of adsorbent dose on percentage removal of nitrate from aqueous solution with HTlc used in this study is graphically shown in Fig. 7. It is evident from the figure that the removal of nitrate increased from 66.6% to 84.6%, 60.4% to 79.8% and 54.5% to 74.7% for 0.1 to 0.8 g of Ca–Al–Cl HTlc in 100 mL of synthetic solution of initial nitrate concentration, 10 mg/L, 50 mg/L and 100 mg/L, respectively. However it is observed that after dosage of 0.35 g, there was no significant change in percentage removal of nitrate. This may be due to the overlapping of active sites at higher dosage. So, there was not any appreciable increase in the effective surface area resulting due to the conglomeration of

Fig. 5. XRD pattern of Ca–Al–Cl layered double hydroxide before and after adsorption.

Table 3
Removal of nitrate from ground water samples collected from different bore wells.

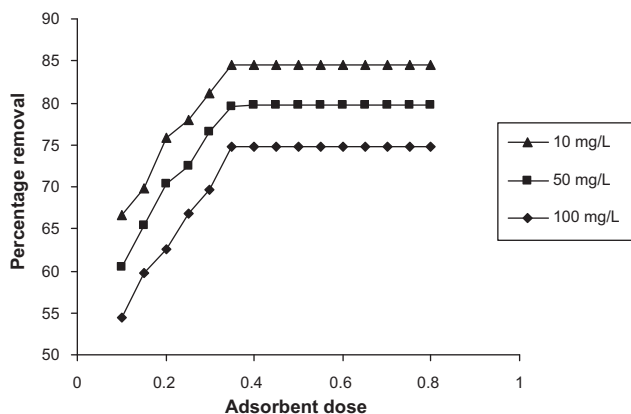| Water samples	Initial nitrate concentration (mg/L)	Final nitrate concentration (mg/L)	Percentage removal
Sample – 1	68.9	15.2	77.9
Sample – 2	88.2	21.1	76.1
Sample – 3	30.2	5.6	81.4
Sample – 4	91.1	22.8	74.9
Sample – 5	70.8	14.9	78.9
Sample – 6	136.8	41.6	69.6

Fig. 7. Adsorbent dose versus percentage removal of nitrate by Ca–Al–Cl LDH with initial concentration of 10 mg/L, 50 mg/L and 100 mg/L.

adsorbent particles [37]. So, 0.35 g in 100 mL of synthetic nitrate solution was considered as optimum dose and was used for further study.

3.2.2. Effect of pH

Percentage removal of nitrate was studied at ambient temperature ($25 \pm 2\,^\circ$C) and contact time of 30 min for initial nitrate concentration of 10 mg/L, 50 mg/L and 100 mg/L at different pH. The result is presented in Fig. 8. It is evident from the figure that the percentage removal of nitrate by Ca–Al–Cl HTlc decreased from 84.5% to 76.9%, 79.8% to 72.6% and 74.7% to 66.5% for increase in pH from 6 to 12, for initial nitrate concentration of 10 mg/L, 50 mg/L and 100 mg/L, respectively. It is evident from the above data and figures that there was slight decrease (7–8%) in percentage removal with increase in pH of the solution. This may be due to the fact that with increase in pH, OH^- concentration in the solution increases, which competes with nitrate ion. The above data suggests that the optimum pH for removal of nitrate was 6.

3.2.3. Effect of contact time

Adsorption of nitrate at different contact time was studied for initial nitrate concentration of 10 mg/L, 50 mg/L and 100 mg/L keeping all other parameters constant. The result is presented in Fig. 9. The percentage removal when Ca–Al–Cl HTlc used, was found to increase from 34.5% to 84.5%, 29.6% to 79.6% and 24.9% to 74.7% for 5 min to 40 min of contact time and initial nitrate concentration of 10 mg/L, 50 mg/L and 100 mg/L, respectively. It is clear from the figure that about 30% removal took place within first 5 min and equilibrium was established after 40 min. Change in rate of removal might be due to the fact that initially chloride ion was present in
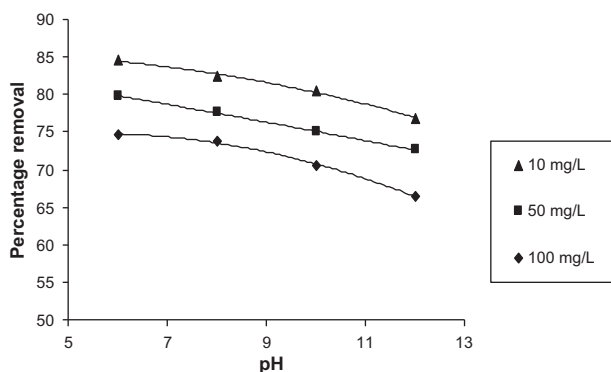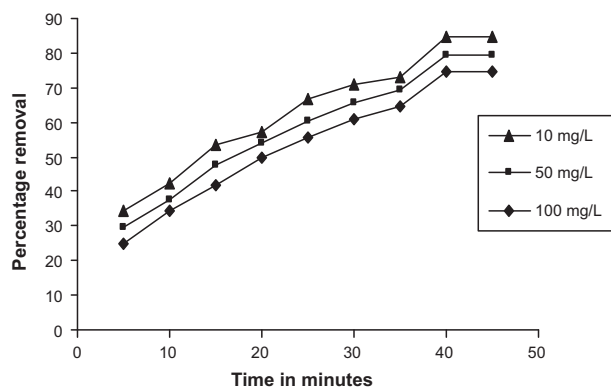

Fig. 9. Time versus percentage removal of lead, Ca–Al–Cl LDH, with initial concentration of 10 mg/L, 50 mg/L and 100 mg/L.

all adsorbent sites and the solute concentration gradient was high. Later, the nitrate uptake rate by adsorbent was decreased significantly, due to the decrease in number of replaceable chloride ions in adsorption sites as well as decrease in nitrate concentration. Decreased removal rate, particularly, towards the end of experiments, indicates the possible monolayer formation of lead ion on the outer surface.

3.2.4. Adsorption kinetics

Determination of efficiency of adsorption process requires an understanding of the time dependence of the concentration distribution of the solute in both bulk solution and solid adsorbent or the kinetics of the process and identification of the rate determining step. Adsorption of nitrate ion was rapid for the first 5 min and its rate slowed down as the equilibrium approached. Rate constant K_{ad} for sorption of nitrate was studied by Lagergren rate equation [38,39] for initial lead concentration of 10 mg/L, 50 mg/L and 100 mg/L.

$$log(q_e - q) = \log q_e - K_{ad} \left(\frac{t}{2.303} \right) \tag{i}$$

where q_e and q (both in mg/g) are the amounts of nitrate adsorbed at equilibrium and at time 't', respectively. The plots of $log(q_e - q_t)$ versus 't' at different time intervals were almost linear, indicating the validity of Lagergren rate equation of first order kinetics (Fig. 10). The adsorption rate constant (K_{ad}), calculated from the slope of the above plot is presented in Table 4.

3.2.5. Intraparticle diffusion rate constant

In order to test the existence of intraparticle diffusion in the adsorption process, the amount of nitrate sorbed per unit mass of adsorbents, q_e at any time t, was plotted as a function of square
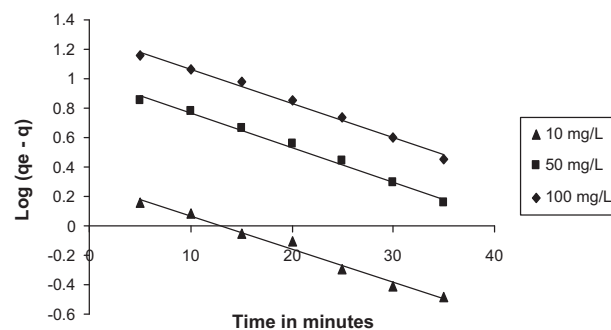

Fig. 8. Percentage removal of nitrate by Ca–Al–Cl LDH of initial concentration, 10 mg/L, 50 mg/L and 100 mg/L versus pH of the synthetic solution.

Fig. 10. Linear plot of Lagergren rate equation using Ca–Al–Cl LDH, time versus log ($q_e - q$) with initial lead concentration of 10 mg/L, 50 mg/L and 100 mg/L.

Table 4
Rate constants (K_{ad}) obtained from the graph for HTlc with different initial concentrations of nitrate.

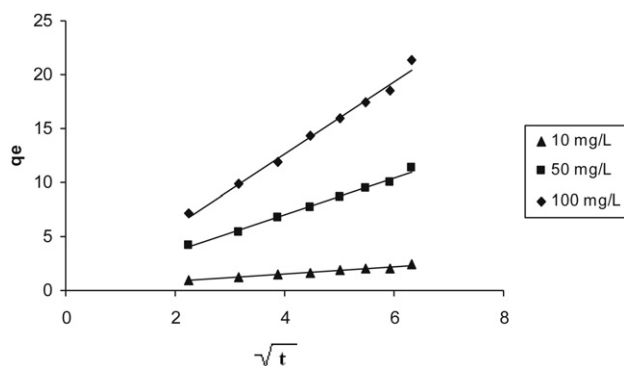| Initial concentration (mg/L)	Slope	Intercept	Rate constant in min^{-1} (K_{ad})	R^2
10	−0.02234	0.28909	0.05147	0.993
50	−0.02343	1.00271	0.05397	0.992
100	−0.02332	1.29815	0.05370	0.991

Fig. 11. Linear plot of Weber–Morris equation using Ca–Al–Cl LDH, square root of time versus q_e with initial nitrate concentration of 10 mg/L, 50 mg/L and 100 mg/L.
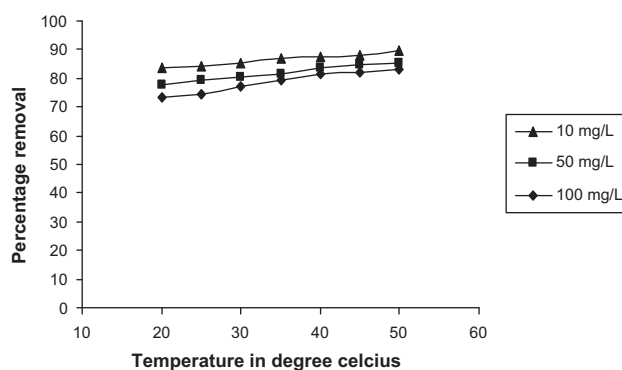

Fig. 12. Temperature versus percentage removal of nitrate with Ca–Al–Cl LDH, initial nitrate concentration of 10 mg/L, 50 mg/L and 100 mg/L.

root of time ($t^{1/2}$). The rate constant for intraparticle diffusion was obtained using Weber–Morris equation given as follows [40],

$$q_e = K_p t^{1/2} + C \tag{ii}$$

where q_e is the amount of nitrate adsorbed in mg/g, K_p is the intraparticle diffusion rate constant and 't' is the agitation time in minutes. Due to stirring there is a possibility of transport of nitrate species from the bulk into pores of the HTlc as well as adsorption at outer surface of the HTlc. The rate-limiting step may be either adsorption or intraparticle diffusion.

In order to study the diffusion process, batch adsorption experiments were carried out with HTlc at ambient temperature (25 ± 2 °C) with initial nitrate concentration of 10 mg/L, 50 mg/L and 100 mg/L. The results obtained are presented in Table 5 and graphically shown in Fig. 11. The rate constants (K_p) for intraparticle diffusion for various initial concentrations of nitrate solution were determined from the slope of respective plots. It is evident from the graph that, the plots were straight lines but the y-intercepts of the plot were non-zero (not passing through the origin) thus indicating that intraparticle diffusion is not the sole rate-limiting factor for the adsorption of nitrate onto HTlc. The values of K_p in Table 5 show the increase in K_p with the increase in nitrate concentration. So, it can be related to concentration diffusion [41].

3.2.6. Effect of temperature

The effect of temperature on the adsorption of nitrate with initial concentration 10 mg/L, 50 mg/L and 100 mg/L onto Ca–Al–Cl HTlc was studied using optimum adsorbent dose and the results are presented as percentage removal of nitrate versus temperature (Fig. 12). The percentage removal of nitrate with initial concentration 10 mg/L, increased from 83.5% to 89.5%, the percentage removal of nitrate with initial concentration 50 mg/L, increased from 77.8% to 85.5% and the percentage removal of nitrate with initial concentration 100 mg/L, increased from 73.4% to 82.9% for 20 °C to 50 °C temperature. It can be clearly seen from the figure that, at the temperature of 20 °C the removal was more that 70% and with increase in temperature, the percentage removal increased slowly and reached almost 90% (initial nitrate concentration of 10 mg/L), which indicates the endothermic nature of the process.

Calculating thermodynamic parameters further supported this. The change in free energy (ΔG), enthalpy (ΔH) and entropy (ΔS) of adsorption were calculated using the following equations [38,39].

$$\log K_C = \frac{\Delta S}{2.303R} - \frac{\Delta H}{2.303RT} \tag{iii}$$

$$\Delta G = \Delta H - T\Delta S \tag{iv}$$

where ΔS and ΔH are the changes in entropy and enthalpy of adsorption, respectively. A plot of $\log K_C$ versus $1/T$ for initial nitrate concentration of 10 mg/L, 50 mg/L and 100 mg/L was linear (Fig. 13). Values of ΔH and ΔS were evaluated from the slope and intercept of Van't Hoff plots and represented in Table 6. The positive values of ΔS indicate some structural changes in the adsorbent and also reflect the affinity of the adsorbent for nitrate species. The positive value of entropy (ΔS) indicates the increase in randomness of the ongoing. During the adsorption of nitrate, the chloride ions (which are displaced by the nitrate ions) gain more entropy than is lost by adsorbate species, thus increasing the randomness in the system. Negative value of ΔG at each temperature indicates the spontaneity of ongoing adsorption. A decrease in values of ΔG with the increase in temperature suggests more adsorption of nitrate at higher temperature. The endothermic nature of the process was once again confirmed by the positive value of enthalpy (ΔH). Positive value of enthalpy (ΔH) suggests that entropy is responsible for making the ΔG value negative. So, the adsorption process was spontaneous, since the entropy contribution was much larger than that of enthalpy.
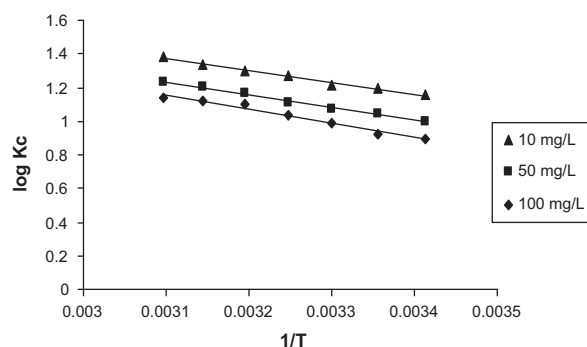

Fig. 13. Van't Hoff plots, $\log K_C$ versus $1/T$ for Ca–Al–Cl LDH, initial nitrate concentration of 10 mg/L, 50 mg/L and 100 mg/L.

Table 5
Intraparticle diffusion rate constants obtained from Weber–Morris equation for different initial concentrations of nitrate.

Initial concentration (mg/L)	Slope	Intercept	Rate of pore diffusion (K_p)	R^2
10	0.33282	0.202929	0.33282	0.985
50	1.67014	0.30958	1.67014	0.991
100	3.30083	−0.53757	3.30083	0.992

Table 6
Thermodynamic parameters using Ca–Al–Cl HTlc, synthetic nitrate solution of 10 mg/L, 50 mg/L and 100 mg/L.

Initial nitrate concentration (mg/L)	ΔH (kJ/mol)	ΔS (kJ/mol)	ΔG (kJ/mol)							R^2
			20 °C	25 °C	30 °C	35 °C	40 °C	45 °C	50 °C	
10	13.52618	0.06820	−0.987	−1.560	−2.133	−2.706	−3.280	−3.853	−4.426	0.986
50	14.29281	0.06787	−1.231	−1.797	−2.364	−2.930	−3.496	−4.062	−4.628	0.986
100	15.95060	0.07156	−1.789	−2.294	−2.798	−3.303	−3.808	−4.313	−4.817	0.981

3.2.7. Effect of initial concentration

To investigate the effect of initial nitrate concentration on nitrate adsorption onto Ca–Al–Cl HTlc, batch mode experiments were performed at ambient temperature (25 ± 2 °C). The initial concentration of nitrate solution was varied from 10 mg/L to 100 mg/L with optimum adsorbent dose. The result obtained is presented in graphical form as percentage removal versus initial nitrate concentration (Fig. 14). It is evident from the graph that the percentage removal of nitrate decreased from 84.5% to 74.7% for initial nitrate concentration of 10 mg/L to 100 mg/L. The results indicate that there is a reduction in nitrate adsorption, owing to the lack of available active sites required for the high initial concentration of nitrate. The adsorbent dose was constant at 0.35 g in 100 mL synthetic nitrate solution of different initial concentrations. With increase in the initial nitrate concentration, the amount of adsorbate species in the solution increases but the amount of adsorbent remains constant and hence the percentage removal decrease with increase in initial nitrate concentration. The higher uptake of nitrate at low concentration may be attributed to the availability of more active sites on for lesser number of adsorbate species.

3.2.8. Adsorption isotherm

The adsorption data were fitted to linearly transformed Langmuir adsorption isotherm. The linearized Langmuir equation, which is valid for monolayer sorption onto a surface with finite number of identical sites, is given by the following equation [38,39].

$$\frac{1}{q_e} = \frac{1}{q_0 b C_e} + \frac{1}{q_0} \qquad (v)$$

where q_0 is the maximum amount of the nitrate ion per unit weight of Ca–Al–Cl HTlc to form a complete monolayer on the surface (adsorption capacity), C_e denotes equilibrium adsorbate concentration in solution, q_e is the amount adsorbed per unit mass of adsorbent, and b is the binding energy constant. The linear plot of
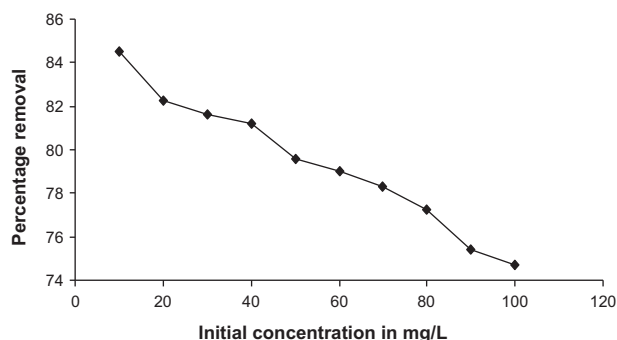
$1/C_e$ versus $1/q_e$ (Fig. 15) with $R^2 = 0.997$ indicates the applicability of Langmuir adsorption isotherm. The values of Langmuir parameters, q_0 and b are 37.65740 mg/g and 0.04344 L/mg, respectively.

In order to predict the adsorption efficiency of the adsorption process, the dimensionless equilibrium parameter was determined by using the following equation [38,39].

$$r = \frac{1}{1 + bC_o} \qquad (vi)$$

where C_o is the initial concentration. Values of $r < 1$ represent favorable adsorption. The r-value for initial concentration of 10 mg/L, 50 mg/L and 100 mg/L was found to be 0.69715, 0.31525 and 0.18712, respectively. The values indicated a favorable system.

It is known that the Langmuir and Freundlich adsorption isotherm constant do not give any idea about the adsorption mechanism. In order to understand the adsorption type, equilibrium data were tested with Dubinin–Radushkevich isotherm [38]. The linearized D–R equation can be written as;

$$\ln q_e = \ln q_m - K\varepsilon^2 \qquad (vii)$$

where ε is Polanyi potential, and is equal to $RT \ln(1 + 1/C_e)$, q_e is the amount of nitrate adsorbed per unit mass of adsorbent, q_m is the theoretical adsorption capacity, C_e is the equilibrium concentration of nitrate, K is the constant related to adsorption energy, R is universal gas constant and T is the temperature in Kelvin scale.

Fig. 16 shows the plot of $\ln q_e$ against ε^2, which was almost linear with correlation coefficient, $R^2 = 0.949$. D–R isotherm constants K and q_m were calculated from the slope and intercept of the plot, respectively. The value of K was found to be 0.00416 mol^2 kJ^{-2} and that of q_m was 0.01914 g/g. The mean free energy of adsorption (E) was calculated from the constant K using the relation [39].
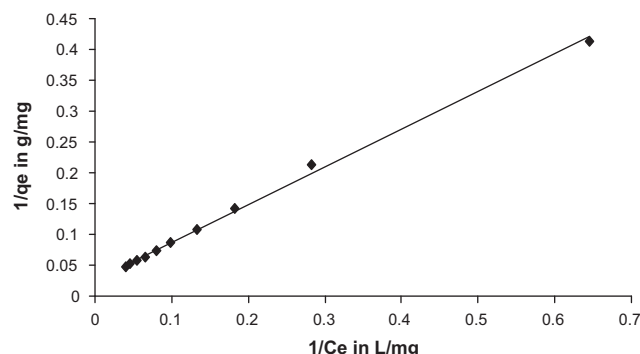
$$E = (2K)^{-1/2} \qquad (viii)$$

Fig. 14. Percentage removal of nitrate by Ca–Al–Cl LDH versus initial nitrate concentration.

Fig. 15. Langmuir adsorption isotherm, $1/C_e$ versus $1/q_e$ for Ca–Al–Cl LDH.
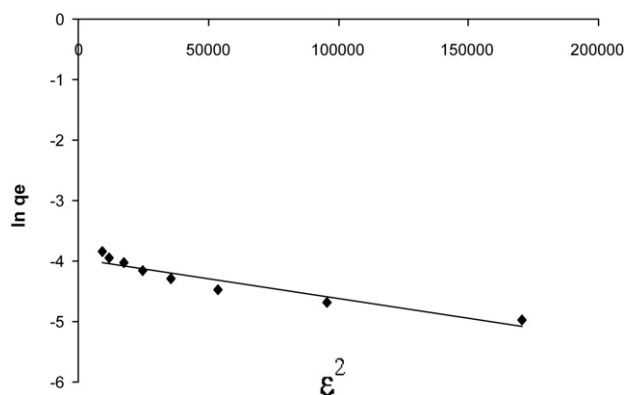
Fig. 16. D–R adsorption isotherm, $\ln q_e$ versus ε^2 for Ca–Al–Cl LDH.

It is defined as the free energy change when 1 mol of ion is transferred to the surface of the solid from infinity in solution. The value of E was found to be 10.95 kJ mol^{-1}. The value of E is very useful in predicting the type of adsorption and if the value is less than 8 kJ mol^{-1}, then the adsorption is physical in nature and if it is in between 8 and 16 kJ mol^{-1}, then the adsorption is due to exchange of ions [39]. The value found in the present study was in between 8 and 16 kJ mol^{-1}. So, the adsorption can be best explained as exchange of ions.

3.2.9. Effect of competitive ions

Till now all the adsorption results discussed above were obtained taking nitrate ion only. However, in reality the nitrate contaminated water contains several other anions which can equally compete in the adsorption process. In order to see effect of interfering ions on adsorption of nitrate, a mixture of known quantities commonly occurring anions in water, viz., phosphate, chloride, carbonate, bicarbonate and sulphate were added to nitrate solutions. The initial concentration of nitrate was fixed at 10 mg/L, 50 mg/L and 100 mg/L while the initial concentration of other anions varied from 10 mg/L to 100 mg/L. The dependence of such ions on adsorption of nitrate at varying concentrations of competitive anions is shown in Fig. 17. It was clear from the figure that presence of these anions reduced the adsorption of nitrate appreciably. The anions reduced the nitrate adsorption in the order of, carbonate > bicarbonate > phosphate > chloride > sulphate. From the above discussion, it is evident that carbonate has maximum and sulphate has least effect on the removal of nitrate by Ca–Al–Cl HTlc. It is evident from the figure that the effect of carbonate and bicarbonate on the removal of nitrate was almost the same. It was observed that the percentage removal of nitrate was reduced by >25% by carbonate and bicarbonate. This may be due to the fact that HTlcs have a strong affinity for carbonate and hence they have a tendency to form corresponding carbonates. It was also observed that, sulphate and chloride exhibited similar effect. Both sulphate and chloride reduced the percentage removal of nitrate by <15%. It may be concluded that Ca–Al–Cl HTlc can be efficiently utilized to remove nitrate from water containing high concentrations of sulphates and chlorides. Nitrate removal by Ca–Al–Cl HTlc may face some difficulties if the concentration of carbonate and bicarbonate (alkalinity) in the water is high. So, the alkalinity of the water is to be analyzed before the removal of nitrate by Ca–Al–Cl HTlc is carried out.

3.2.10. Desorption and regeneration studies

Desorption and regeneration studies give an idea about the nature of adsorption. Normally, chemisorption exhibits poor desorption. It may be due to the fact that in chemisorption the adsorbate species are held firmly to the adsorbent with comparatively stronger bonds. Regeneration study was carried out in order
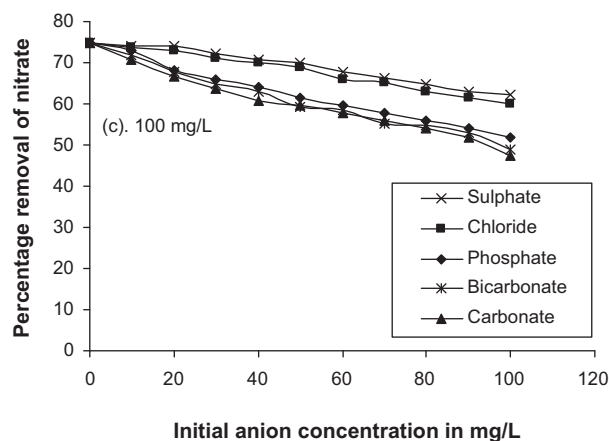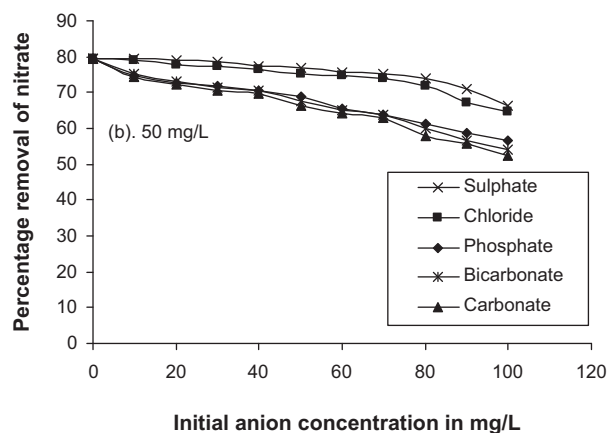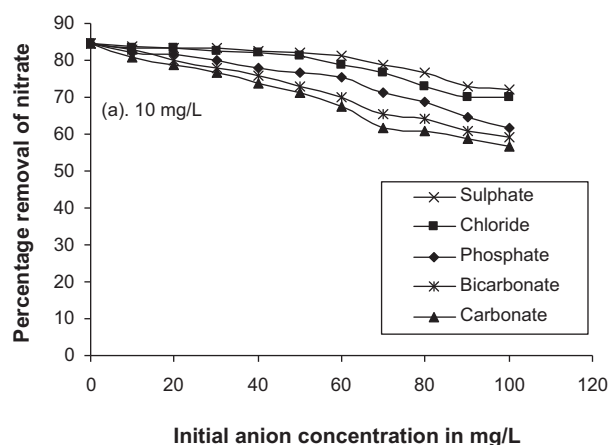

Fig. 17. Percentage removal versus initial anion concentration of solution with initial nitrate concentration of (a) 10 mg/L, (b) 50 mg/L and (c) 100 mg/L.

to know the reusability of the adsorbent. The result of the study is presented in Table 7. Desorption of the adsorbed nitrate in neutral distilled water resulted about 2.31%, 2.33% and 2.22% for initial concentration of 10 mg/L, 50 mg/L and 100 mg/L, respectively. It is evident from the low desorption values, that the adsorption of nitrate onto HTlc was chemical in nature, which is in good agreement with the previous data obtained from free energy study.

At the end of the adsorption process, when the working capacity of an adsorbent is exhausted, it has to be regenerated. Adsorbents are usually regenerated with acid or alkali solution. In the present study, adsorbent (HTlc) was unstable in acidic medium. So, the regeneration study was carried out at pH of 8, 10 and 12. It was
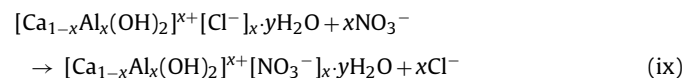
Table 7
Percentage desorption and regeneration of nitrate of different concentration by Ca–Al–Cl HTlc at varying pH.

Initial nitrate concentration (mg/L)	Amount adsorbed (%)	Amount desorbed (%)				Percentage desorption or regeneration			
		pH – 8	pH – 10	pH – 12	Distilled water	pH – 8	pH – 10	pH – 12	Distilled Water
10	84.5	2.01	2.03	2.05	1.96	2.37	2.40	2.42	2.31
50	79.8	1.89	1.93	1.95	1.86	2.36	2.41	2.44	2.33
100	74.7	1.70	1.73	1.80	1.66	2.27	2.31	2.40	2.22

observed from Table 7 that regeneration was less than 3% at different pH. So, once HTlc-nitrate is formed it is difficult to regenerate.

3.2.11. Mechanism of nitrate removal

Anion replacement involves the breaking up of the electrostatic interactions as well as the hydrogen bonds between the hydroxide layers and the outgoing anion and the reformation of these bonds with the incoming anions. Diffraction peaks of nitrate containing material were found in the XRD analysis (Fig. 5) of HTlc obtained after nitrate adsorption. This may be due to nitrate uptake by the material. The HTlc used in the present study contains intercalated chloride ions. When the HTlc is added to the synthetic nitrate solution, the chloride ion of the HTlc is replaced by nitrate ions [42]. And hence an HTlc with intercalated nitrate ion is formed leaving behind chloride ions in the solution. In addition to replacement of chloride ions by nitrate ions, there is a possibility of physical adsorption of nitrate ions by the HTlc. The most probable general mechanism for anion replacement reaction in HTlc can be suggested as below:

$$[Ca_{1-x}Al_x(OH)_2]^{x+}[Cl^-]_x \cdot yH_2O + xNO_3^-$$
$$\rightarrow [Ca_{1-x}Al_x(OH)_2]^{x+}[NO_3^-]_x \cdot yH_2O + xCl^- \qquad (ix)$$

Mikami et al. (1984) have studied the anion replacement reactions of Ni–Al–Cl HTlc and suggested similar mechanism [42]. Sasaki et al. (1982) also reported similar anion replacement mechanism [43]. They propose a two-step mechanism involving the adsorption of the incoming ions followed by the 'desorption' of the Cl⁻ ions. Kooli et al. (1997) have measured the conductivity during vanadate replacement in the Mg–Al–Cl LDH and they propose first order kinetics involving direct anion replacement [44].

4. Conclusion

Ca–Al–Cl hydrotalcite was synthesized by calcium chloride, aluminum chloride, sodium chloride and sodium hydroxide by co precipitation method. Synthesis was ascertained by adopting various characterizing methods like SEM, XRD, FTIR, TGA–DSC and chemical analysis. Ca–Al–Cl hydrotalcite exhibited much greater specific surface area and which increased with increase in calcination temperature. The adsorption of nitrate from aqueous solution by Ca–Al–Cl hydrotalcite was found to occur readily. The material was found to exhibit good adsorption efficiency. Adsorption of nitrate was found to follow first order kinetics. The effect of other anions were also studied and was found that the anions reduced the nitrate adsorption in the order of carbonate > phosphate > chloride > sulphate. The percentage removal was found to decrease with increase in pH. A regeneration study of the material was also carried out and was found that the Ca–Al–Cl hydrotalcite cannot be easily regenerated and reused. The percentage regeneration was less than 2%. The removal of nitrate with Ca–Al–Cl hydrotalcite was very efficient and can bring down the nitrate concentration to its permissible limit. The process can be employed as a primary step for the removal of nitrate to meet permissible limit of nitrate in surface and ground water.

References

[1] W. Meng, F. Li, D.G. Evans, X. Duan, Preparation and intercalation chemistry of magnesium–iron(III) layered double hydroxides containing exchangeable interlayer chloride and nitrate ions, Mater. Res. Bull. 39 (9) (2004) 1185–1193.
[2] Y. Li, B. Gao, T. Wu, W. Chen, X. Li, B. Wang, Adsorption kinetics for removal of thiocyanate from aqueous solution by calcined hydrotalcite, Colloids Surf. A: Physicochem. Eng. Aspects 325 (1–2) (2008) 38–43.
[3] B.M. Choudary, M.L. Kantam, A. Rahman, C. Reddy, V. Reddy, Selective reduction of aldehydes to alcohols calcined hydrotalcite, J. Mol. Catal. A: Chem. 206 (1–2) (2003) 145–151.
[4] I. Pavlovic, C. Barriga, M.C. Hermosín, J. Cornejo, M.A. Ulibarri, Adsorption of acidic pesticides 2,4-D Clopyralid and Picloram on calcined hydrotalcite, Appl. Clay Sci. 30 (2) (2005) 125–133.
[5] E. Álvarez-Ayuso, H.W. Nugteren, Purification of chromium(VI) finishing wastewaters using calcined and uncalcined Mg–Al–CO₃-hydrotalcite, Water Res. 39 (12) (2005) 2535–2542.
[6] A. Sugier, E. Freund, U.S. Patent 4,112,110, Institut Francais du Petrole (1978).
[7] I. Chatti, A. Ghorbel, P. Grange, J.M. Colin, Oxidation of mercaptans in light oil sweetening by cobalt(II) phthalocyanine-hydrotalcite catalysts, Catal. Today 75 (1–4) (2002) 113–117.
[8] K. Nishida, I. Atake, D. Li, T. Shishido, Y. Oumi, T. Sano, K. Takehira, Effects of noble metal-doping on Cu/ZnO/Al₂O₃ catalysts for water–gas shift reaction: catalyst preparation by adopting "memory effect" of hydrotalcite, Appl. Catal. A 337 (1) (2008) 48–57.
[9] P. Kuśtrowski, D. Sułkowska, L. Chmielarz, R. Dziembaj, Aldol condensation of citral and acetone over mesoporous catalysts obtained by thermal and chemical activation of magnesium–aluminum hydrotalcite like precursors, Appl. Catal. A 302 (2) (2006) 317–324.
[10] D. Tichit, D. Lutic, B. Coq, R. Durand, R. Teissier, The aldol condensation of acetaldehyde and heptanal on hydrotalcite-type catalysts, J. Catal. 219 (1) (2003) 167–175.
[11] B.M. Choudary, M. Lakshmi Kantam, B. Kavita, C.V. Reddy, F. Figueras, Catalytic C–C bond formation promoted by Mg–Al–O–t-Bu hydrotalcite, Tetrahedron 56 (47) (2000) 9357–9364.
[12] F.A. Khan, J. Dash, R. Satapathy, S.K. Upadhyay, Hydrotalcite catalysis in ionic liquid medium: a recyclable reaction system for heterogeneous Knoevenagel and nitroaldol condensation, Tetrahedron Lett. 45 (15) (2004) 3055–3058.
[13] Y. Li, B. Gao, T. Wu, W. Chen, X. Li, B. Wang, Adsorption kinetics for removal of thiocyanate from aqueous solution by calcined hydrotalcite, Colloids Surf. A 325 (1–2) (2008) 38–43.
[14] D.P. Das, J. Das, K. Parida, Physicochemical characterization and adsorption behavior of calcined Zn/Al hydrotalcite-like compound (HTlc) towards removal of fluoride from aqueous solution, J. Colloid Interface Sci. 261 (2) (2003) 213–220.
[15] O.P. Ferreira, S.G. de Moraes, N. Durán, L. Cornejo, O.L. Alves, Evaluation of boron removal from water by hydrotalcite-like compounds, Chemosphere 62 (1) (2006) 80–88.
[16] P.F. Hudak, Regional trends in nitrate content of Texas groundwater, J. Hydrol. 228 (2000) 37–47.
[17] G.D. Agrawal, S.K. Lunkad, T. Malkhed, Diffuse agricultural nitrate pollution of ground waters in India, Water Sci. Technol. 39 (1999) 67–75.
[18] M.N. Almasri, J.J. Kaluarachchi, Assessment and management of longterm nitrate pollution of ground water in agriculture-dominated watersheds, J. Hydrol. 295 (2004) 225–245.
[19] A.H. Wolfe, J.A. Patz, Reactive nitrogen and human health: acute and long-term implications, Ambio 31 (2002) 120–125.
[20] US Environmental Protection Agency, Drinking water standards and health 614 advisories, US Environmental Protection Agency, Office of Water, 2000, 822-B-00-001.

[21] A. Agrawal, P.G. Tratnyek, Reduction of nitro aromatic compounds by zero-valent iron metal, Environ. Sci. Technol. 30 (1996) 153–160.

[22] F. Cheng, R. Muftikian, Q. Fernando, N. Korte, Reduction of nitrate to ammonia by zero valent iron, Chemosphere 35 (1997) 2689–2695.

[23] Y.H. Huang, T.C. Zhang, Effects of low pH on nitrate reduction by iron powder, Water Res. 38 (2004) 2631–2642.

[24] Y.H. Huang, T.C. Zhang, Kinetics of nitrate reduction by iron at near neutral pH, J. Environ. Eng. 128 (2002) 604–610.

[25] Y. Chen, C. Li, S. Chen, Fluidized zero valent iron bed reactor for nitrate removal, Chemosphere 59 (2005) 753–759.

[26] J. Kielemoes, P. de Boever, W. Verstraete, Influence of denitrification on the corrosion of iron and stainless steel powder, Environ. Sci. Technol. 34 (2000) 663–671.

[27] J.C. Fanning, The chemical reduction of nitrate in aqueous solution, Coord. Chem. Rev. 199 (2000) 159–179.

[28] A. Kapoor, T. Viraraghavan, Nitrate removal from drinking water—review, J. Environ. Eng. 123 (1997) 371–380.

[29] D.P. Das, J. Das, K. Parida, Physicochemical characterization and adsorption behavior of calcined Zn/Al hydrotalcite-like compound (HTlc) towards removal of fluoride from aqueous solution, J. Colloid Interface Sci. 261 (2003) 213–220.

[30] A.I. Vogel, A Text Book of Quantitative Inorganic Analysis, Longman, London, 1969, pp. 433–434.

[31] G. Allegra, G. Ronca, Crystal powder statistics. II. Line profiles in diffraction spectra of identical crystals and of Gaussian samples, crystal size distributions, Acta Cryst. A34 (1978) 1006–1013.

[32] D. Roy, R. Roy, E. Osborn, The system $MgO–Al_2O_3–H_2O$ and influence of carbonate and nitrate ions on the phase equilibria, Am. J. Sci. 251 (1953) 337–361.

[33] R. Allmann, Double layer structures with brucite-like ions $[Me(II)_{(1−x)}Me(III)_x(OH)_2]^{x+}$, Chimia 24 (3) (1970) 99–108.

[34] R.S. Zhai, A. Das, C.-K. Hsu, C.C. Han, T. Canteenwala, L.Y. Chiang, T.J. Chuang, Polymeric fullerene oxide films produced by decomposition of hexanitro[60]fullerene, Carbon 42 (2004) 395–403.

[35] B.J. Hathway, A.E. Underhill, The infrared spectra of some transition-metal perchlorates, J. Chem. Soc. (1961) 3091–3096.

[36] J.T. Kloprogge, L. Hickey, R.L. Frost, The effect of varying synthesis conditions on zinc chromium hydrotalcite: a spectroscopic study, Mater. Chem. Phys. 89 (1) (2005) 99–109.

[37] H. Tahir, Comparative trace metal contents in sediments and the removal of chromium using Zeolite-5A, EJEAF Che 4 (4) (2005) 1021–1032.

[38] M. Islam, R.K. Patel, Evaluation of removal efficiency of fluoride from aqueous solution using quick lime, J. Hazard. Mater. 143 (2007) 303–310.

[39] M. Islam, R.K. Patel, Polyacrylamide thorium (IV) phosphate as an important lead selective fibrous ion exchanger: synthesis, characterization and removal study, J. Hazard. Mater. 156 (2008) 509–520.

[40] A.K. Yadav, C.P. Kaushik, A.K. Haritash, A. Kansal, N. Rani, Defluoridation of groundwater using brick powder as an adsorbent, J. Hazard. Mater. 128 (2–3) (2006) 289–293.

[41] K. Kadirvelu, C. Faur-Brasquet, P. Le-Cloiree, Removal of Cu(II), Pb(II) and Ni(II) by adsorption onto activated carbon cloths, Langmuir 16 (2000) 8404–8409.

[42] N. Mikami, M. Sasaki, S. Horibe, T. Yasunaga, Kinetic study of ion exchange of phosphate ions for chloride in a hydrotalcite-like compound, $Ni_{0.75}Al_{0.25}(OH)_2Cl_{0.25}·mH_2O$, using the pressure-jump technique, J. Phys. Chem. 88 (1984) 1716–1719.

[43] M. Sasaki, N. Mikami, T. Ikeda, K. Hachiya, T. Yasunaga, Kinetic studies on intercalation–deintercalation of hydroxide and chloride in a hydrotalcite-like compound; $Ni_{0.75}Al_{0.25}(OH)_2Cl_{0.25}$ using the pressure-jump technique, J. Phys. Chem. 86 (1982) 4413–4417.

[44] F. Kooli, M.J. Holgado, V. Rives, S. Sanroman, M.A. Ulibarri, A simple conductivity study of decavanadate intercalation in hydrotalcite, Mater. Res. Bull. 32 (1997) 977–982.